DALTON
FULL PAPER

Ca^{2+}–Fe^{3+}–D-gluconate-complexes in alkaline solution. Complex stabilities and electrochemical properties

Thomas Bechtold, Eduard Burtscher and Aurora Turcanu

Institute of Textile Chemistry and Textile Physics, Leopold-Franzens-University Innsbruck, A-6850 Dornbirn, Austria. E-mail: textilchemie@uibk.ac.at

Received 27th February 2002, Accepted 22nd April 2002
First published as an Advance Article on the web 22nd May 2002

The complexation of Fe^{3+} and Ca^{2+} ions by D-gluconate (DGL) in alkaline solutions was studied by potentiometric titration. Stability constants for the complexes were determined by mathematical treatment of the data with the computer program BEST. Depending on the concentration of ligand, complexes of Fe^{3+} : DGL stoichiometry 1 : 1, 1 : 2 and 2 : 2 were identified. In the presence of Ca^{2+} ions mixed binuclear complexes are formed with the Ca^{2+} : Fe^{3+} : DGL stoichiometries 1 : 1 : 1 and 1 : 1 : 2. The complex system was studied with cyclic voltammetry and with constant current electrolysis experiments. The uptake of Ca^{2+} into the Fe^{III}DGL complexes results in a distinct change of the electrochemical properties of the iron(II/III)-redox couple. A shift of the formal redox potential towards more negative values is observed. The Ca^{2+} : Fe^{3+} : DGL complexes can be regarded as models for an iron(II/III)-redox system whose electrochemical behaviour is determined by the concentration of an electrochemically inactive ion.

Introduction

Iron-complexes with saccharic acids are of importance in numerous different applications *e.g.* in corrosion inhibition,[1,2] as complexing agents in textile auxiliaries[3,4] and in biological systems.[5] Iron(II/III)-complexes with D-gluconate (DGL) have been studied with regard to medical applications[5] and complexes with DGL have been proposed as mediators for indirect electrochemical reduction of dyestuffs in textile dyeing processes.[6–9] Due to their general importance complexes with sugar-type ligands have been investigated in detail.[10–12] The preparation and isolation of such compounds was first achieved by mixing stoichiometric amounts of Fe^{3+}-salts, D-gluconic acid and sodium hydroxide solution.[13] Traube described the isolation of the basic "calcium-ferri-gluconate" $[C_6H_7O_7Fe^{III}]Ca$ after addition of $CaCl_2$ to previously formed $[C_6H_8O_7Fe^{III}]$-Na. Adding an excess of D-gluconic acid the readily soluble "calcium-ferri-digluconate" $[C_{12}H_{19}O_{14}Fe^{III}]Ca$ was isolated.[13]

Despite the fact that the formation of Fe^{III}DGL complexes has been well known for several decades the scientific data about the composition of the complexes are still contradictory. Pecsok[14] and Escandar[15] describe for alkaline solutions the formation of mononuclear Fe^{III}DGL complexes with a Fe^{3+} : DGL molar ratio of 1 : 1 and various states of deprotonation $[Fe^{III}H_{-x}DGL]^{y+}$ with $0 > x > -4$ and $+2 > y > -2$.[14,15] Nagy investigated solid Fe^{III}DGL complexes by means of spectroscopic methods and described the formation of binuclear species of composition $[Fe^{III}_2H_{-4}DGL_2]Na_2$.[16,17] Gonzales-Velasco proposed mononuclear and binuclear complexes on the basis of ionic mobility measurements with the system Fe^{III}DGL.[18]

In this article investigations describing the complexation of Ca^{2+} by the Fe^{III}DGL system are presented. Formation constants calculated from potentiometric titration experiments with the complex systems Fe^{III}DGL and $CaFe^{III}$DGL are given. The calculations were performed with the computer programm BEST.[19] Such information is required as a basis for a detailed understanding and discussion of the influence of Ca^{2+}-ions on the redox behaviour of Fe^{III}DGL complexes. The uptake of Ca^{2+} into the Fe^{III}DGL complexes results in a distinct change of the electrochemical properties of the $Fe^{III/II}$-redox couple and in a shift of the formal redox potential. The change in the redox behaviour of Fe^{III}DGL due to complexation of Ca^{2+} ions is investigated with CV-experiments and the formal redox potentials were studied in constant current electrolysis experiments with parallel analytical determination of $c(Fe^{2+})$ and $c(Fe^{3+})$.

The data given in this article form a basis for an improved understanding of the electrochemical behaviour of such mixed complex systems formed between Ca^{2+}, Fe^{3+} and sugar type acids.

Experimental

The $Fe(NO_3)_3{\cdot}9H_2O$, $Fe_2(SO_4)_3{\cdot}5–6H_2O$, $Ca(NO_3)_2{\cdot}4H_2O$, $CaCl_2{\cdot}2H_2O$, HNO_3, KNO_3, NaOH, KOH, potassium hydrogen phthalate were analytical grade chemicals (Merck, Riedl-de-Haen). Sodium D-gluconate (NaDGL) with more than 99% purity was used (Merck).

For the determination of complex formation constants the following stock solutions were prepared: $c(Fe(NO_3)_3{\cdot}9H_2O) = 0.01$ mol dm^{-3} in $c(HNO_3) = 0.02$ mol dm^{-3}, $c(DGL) = 0.01$ mol dm^{-3}, $c(Ca(NO_3)_2{\cdot}4H_2O) = 0.01$ mol dm^{-3} and $c(KNO_3) = 1$ mol dm^{-3}. Aliquots of stock solution of ligand, metal ions, KNO_3 and KOH were diluted to the final volume of 50 ml in order to obtain a final concentration of $c(Fe^{3+}) = 1.0 \times 10^{-3}$ mol dm^{-3}, $c(Ca^{2+}) = 1.0 \times 10^{-3}$ mol dm^{-3} and $c(DGL) = 1.2 \times 10^{-3}$ mol dm^{-3} or 2×10^{-3} mol dm^{-3} respectively, with an initial pH of 11.5.

The titrations were perfomed as back titrations with a titroprocessor (Orion Autochemistry System 960, Orion, Boston, MA) using a Hamilton Flushtrode pH-electrode (Hamilton, Bonaduz, CH). The addition of HNO_3 ($c(HNO_3) = 0.1$ mol dm^{-3}) was performed at time intervals of 120 seconds. Titration was performed in the pH-interval between 2 and 11.6 by recording 50 data points. The temperature was maintained at 20 ± 0.1 °C and the ionic strength was adjusted to 0.1 mol dm^{-3} by addition of KNO_3 stock solution.

The KOH solution was standardised against potassium hydrogen phthalate and Gran's plot was carried out to ensure that the base was not contaminated by CO_2. The calibration of the pH-meter readings was performed to read $-\log[H^+]$.

To compare the results of the back titration with the equilibrium measurements, in the case of the Fe^{III}DGL system,

DOI: 10.1039/b202086f

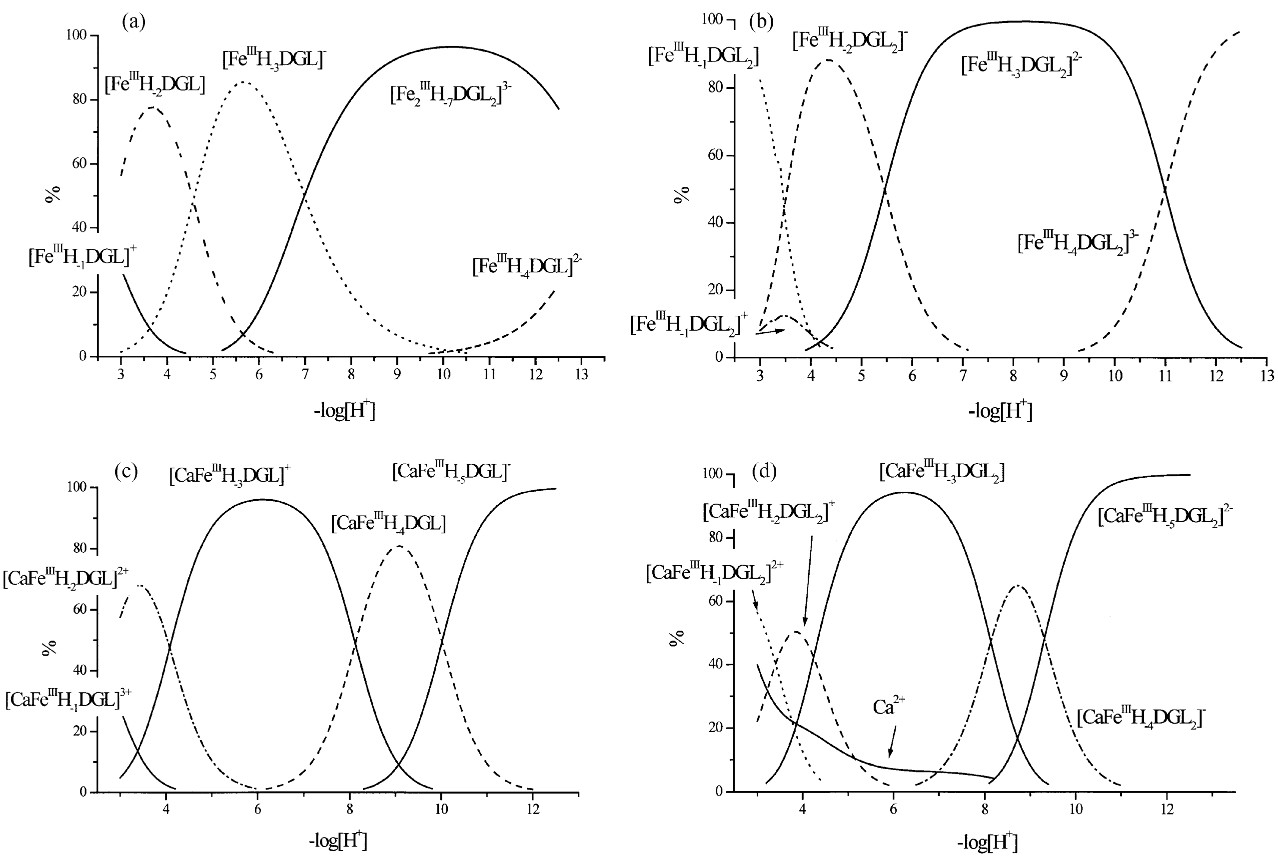

Fig. 1 Species distribution (ionic strength $\mu(KNO_3) = 0.1$ mol dm^{-3}, $T = 20.0 \pm 0.1$ °C) calculated for the system (a) Fe^{III}DGl with a molar ratio 1 : 1 $c(Fe^{3+}) = 0.01$ mol dm^{-3}, c(DGL) = 0.01 mol dm^{-3}; (b) Fe^{III}DGl with a molar ratio 1 : 2, $c(Fe^{3+}) = 0.01$ mol dm^{-3}, c(DGL) = 0.02 mol dm^{-3}; (c) Ca^{2+}Fe^{III}DGl with a molar ratio 1 : 1 : 1 $c(Ca^{2+}) = 0.01$mol dm^{-3}, $c(Fe^{3+}) = 0.01$ mol dm^{-3}, c(DGL) = 0.01 mol dm^{-3}; (d) Ca^{2+}Fe^{III}DGl with a molar ratio 1 : 1 : 2, $c(Ca^{2+}) = 0.01$mol dm^{-3}, $c(Fe^{3+}) = 0.01$ mol dm^{-3}, c(DGL) = 0.02 mol dm^{-3}.

solutions corresponding to 40 different titration points were prepared and pH was measured after a storage time of approx. 48 hours at 20 °C.

The stability constants were calculated using the computer program BEST.[19,20] The quality of the approximation of the measured potentiometric equilibrium curve is given by the parameter σ_{fit} (standard deviation in pH-units[19]). The results are given as formation constants according to the definitions given by Martell.[19]

Potentiometric titration experiments shown in Fig. 2 were performed by adding 0.6 mol dm^{-3} HCl to 100 ml of a solution containing $c(Fe(NO_3)_3{\cdot}9H_2O) = 0.01$ mol dm^{-3}, c(DGL) = 0.02 mol dm^{-3}, c(NaOH) = 0.05 mol dm^{-3} in the presence of $c(CaCl_2)$ 0.01 mol dm^{-3}. Experiments were performed by means of a titroprocessor (Orion Autochemistry System 960, readings 60 s after each increment of HCl).

The CV-experiments were performed at a HMDE-electrode (EG&G potentiostat 264A with 303A polarographic analyser EG&G, Princeton, NJ). The potential values are related to a Ag/AgCl, 3M KCl reference electrode. The investigated mixtures were prepared by mixing defined volumes of solution (A) containing $c(Fe^{3+}) = 0.01$ mol dm^{-3}, c(DGL) = 0.02 mol dm^{-3} and solution (B) containing $c(Fe^{3+}) = 0.01$ mol dm^{-3}, c(DGL) = 0.02 mol dm^{-3} and $c(Ca^{2+}) = 0.01$ mol dm^{-3}. Both solutions A and B, were adjusted to the desired pH by addition of sodium hydroxide solution (c(NaOH) = 0.2 mol dm^{-3}). The detailed composition of the investigated solutions is given in Table 2. The samples were deoxygenated for at least 8 min with N_2. The experiments were performed at room temperature.

The electrochemical reduction experiments were performed in a laboratory scale multi-cathode electrolyser described in more detail in the literature [21,22] (volume of catholyte 1 dm^3, volume of anolyte 0.4 dm^3, anolyte: c(NaOH) 1 mol dm^{-3}; cathode material: stainless steel, cathode area 4320 cm^2, separator: cation exchange membrane 100 cm^2 area, stainless steel anode 100 cm^2 area; cell current 0.6–0.9 A, cathodic current density 0.14–0.2 mA cm^{-2}). The redox potential in the catholyte was measured outside the cell in the catholyte reservoir using a Pt-electrode and a potentiometer (Metrohm, pH meter 654, Metrohm, Herisau, CH). The potential values given are related to a Ag/AgCl, 3M KCl reference electrode. The experiments were performed at room temperature. According to the planned technical application $Fe_2(SO_4)_3{\cdot}5\text{–}6H_2O$, and $CaCl_2{\cdot}2H_2O$ were used as the metal salts. The composition of the catholyte is given below.

The formation of the Fe^{II}-complex and the determination of the total iron concentration were observed with photometry at 520 nm after complexation with 1,10-phenanthroline at pH 4.5.[23]

Results and discussion

Potentiometric titrations: complex stability

As a basis for the study of the CaFe^{III}DGL system a set of stability constants for the complex system Fe^{III}DGL had to be determined as the data given in the literature were not sufficient.[13–18] For the calculations complexes with the Fe^{III}DGL molar ratios 1 : 1, 2 : 1 and 2 : 2 and various states of deprotonation of the complexes were considered.[13–18] The formation of Fe^{3+}–hydroxo species also was considered.[24]

During the calculations a reduction of the relevant species was performed. The stoichiometry of the major species and calculated formation constants are given in Table 1.

The calculated species distribution in a solution containing a Fe^{III}DGL stoichiometry of 1 : 1 is shown in Fig. 1a; in Fig. 1b the species distribution for 1 : 2 stoichiometry is shown.

Table 1 Formation constants and stoichiometry of the formed complexes ($Fe^{III}DGL$ σ_{fit} = 0.015–0.022, $CaFe^{III}DGL$ σ_{fit} = 0.012–0.018), ionic strength 0.1 mol dm^{-3}, 20 °C

		Stoichiometry			
Species	Formation constant (log (β))	Ca^{2+}	Fe^{3+}	H^+	DGL^-
DGLH	3.66	0	0	1	1
$[Fe^{III}DGL]^{2+}$	(10.51)	0	1	0	1
$[Fe^{III}H_{-1}DGL]^+$	9.03	0	1	−1	1
$[Fe^{III}H_{-2}DGL]$	6.35	0	1	−2	1
$[Fe^{III}H_{-3}DGL]^-$	1.78	0	1	−3	1
$[Fe^{III}H_{-4}DGL]^{2-}$	−8.4	0	1	−4	1
$[Fe^{III}DGL_2]^{2+}$	22.23	0	1	0	2
$[Fe^{III}H_{-1}DGL_2]^+$	18.22	0	1	−1	2
$[Fe^{III}H_{-2}DGL_2]^-$	15.30	0	1	−2	2
$[Fe^{III}H_{-3}DGL_2]^{2-}$	9.84	0	1	−3	2
$[Fe^{III}H_{-4}DGL_2]^{3-}$	−1.15	0	1	−4	2
$[Fe^{III}H_{-5}DGL_2]^{4-}$	(−20.0)	0	1	−5	2
$[Fe^{III}{}_2H_{-7}DGL_2]^{3-}$	−1.42	0	2	−7	2
$[CaFe^{III}DGL]^{4+}$	16.26	1	1	0	1
$[CaFe^{III}H_{-1}DGL]^{3+}$	13.89	1	1	−1	1
$[CaFe^{III}H_{-2}DGL]^{2+}$	11.21	1	1	−2	1
$[CaFe^{III}H_{-3}DGL]^+$	7.13	1	1	−3	1
$[CaFe^{III}H_{-4}DGL]$	−0.99	1	1	−4	1
$[CaFe^{III}H_{-5}DGL]^-$	−11.01	1	1	−5	1
$[CaFe^{III}DGL_2]^{3+}$	20.96	1	1	0	2
$[CaFe^{III}H_{-1}DGL_2]^{2+}$	22.47	1	1	−1	2
$[CaFe^{III}H_{-2}DGL_2]^+$	19.06	1	1	−2	2
$[CaFe^{III}H_{-3}DGL_2]$	14.82	1	1	−3	2
$[CaFe^{III}H_{-4}DGL_2]^-$	6.68	1	1	−4	2
$[CaFe^{III}H_{-5}DGL_2]^{2-}$	−2.63	1	1	−5	2
$Fe(OH)^{+}$[a]	−2.9	0	1	−1	0
$Fe(OH)_2{}^{+}$[a]	−6.00	0	1	−2	0
$Fe(OH)_4{}^{-}$[a]	−21.6	0	1	−4	0
$Fe_2(OH)_2{}^{4+}$[a]	−3.0	0	2	−2	0

Species with β value in parentheses are present in very low concentration.[a] Ref. 24.

Stoichiometry: Fe^{3+}:DGL 1:1 **increasing pH**

(1) $DGL^- + H^+ \rightleftarrows DGLH$

(2) $Fe^{3+} + DGL^- \rightleftarrows [Fe^{III}DGL]^{2+}$

(3) $Fe^{3+} + DGL \rightleftarrows [Fe^{III}H_{-1}DGL]^+ + H^+$

(4) $Fe^{3+} + DGL \rightleftarrows [Fe^{III}H_{-2}DGL] + 2H^+$

(5) $Fe^{3+} + DGL \rightleftarrows [Fe^{III}H_{-3}DGL]^- + 3H^+$

(6) $Fe^{3+} + DGL \rightleftarrows [Fe^{III}H_{-4}DGL]^{2-} + 4H^+$

(7) $2Fe^{3+} + 2DGL \rightleftarrows [Fe^{III}{}_2H_{-7}DGL_2]^{3-} + 3H^+$

Ca^{2+}:Fe^{3+}:DGL 1:1:1

(14) $Ca^{2+} + Fe^{3+} + DGL \rightleftarrows [CaFe^{III}DGL]^{4+}$

(15) $Ca^{2+} + Fe^{3+} + DGL \rightleftarrows [CaFe^{III}H_{-1}DGL]^{3+} + H^+$

(16) $Ca^{2+} + Fe^{3+} + DGL \rightleftarrows [CaFe^{III}H_{-2}DGL]^{2+} + 2H^+$

(17) $Ca^{2+} + Fe^{3+} + DGL \rightleftarrows [CaFe^{III}H_{-3}DGL]^+ + 3H^+$

(18) $Ca^{2+} + Fe^{3+} + DGL \rightleftarrows [CaFe^{III}H_{-4}DGL] + 4H^+$

(19) $Ca^{2+} + Fe^{3+} + DGL \rightleftarrows [CaFe^{III}H_{-5}DGL]^- + 5H^+$

Stoichiometry: Fe^{3+}:DGL 1:2 **increasing pH**

(1) $DGL + H^+ \rightleftarrows DGLH$

(8) $Fe^{3+} + 2DGL \rightleftarrows [Fe^{III}DGL_2]^+$

(9) $Fe^{3+} + 2DGL \rightleftarrows [Fe^{III}H_{-1}DGL_2] + H^+$

(10) $Fe^{3+} + 2DGL \rightleftarrows [Fe^{III}H_{-2}DGL_2]^- + 2H^+$

(11) $Fe^{3+} + 2DGL \rightleftarrows [Fe^{III}H_{-3}DGL_2]^{2-} + 3H^+$

(12) $Fe^{3+} + 2DGL \rightleftarrows [Fe^{III}H_{-4}DGL_2]^{3-} + 4H^+$

(13) $Fe^{3+} + 2DGL \rightleftarrows [Fe^{III}H_{-5}DGL_2]^{4-} + 5H^+$

Ca^{2+}:Fe^{3+}:DGL 1:1:2

(20) $Ca^{2+} + Fe^{3+} + 2DGL \rightleftarrows [CaFe^{III}DGL_2]^{3+}$

(21) $Ca^{2+} + Fe^{3+} + 2DGL \rightleftarrows [CaFe^{III}H_{-1}DGL_2]^{2+} + H^+$

(22) $Ca^{2+} + Fe^{3+} + 2DGL \rightleftarrows [CaFe^{III}H_{-2}DGL_2]^+ + 2H^+$

(23) $Ca^{2+} + Fe^{3+} + 2DGL \rightleftarrows [CaFe^{III}H_{-3}DGL_2] + 3H^+$

(24) $Ca^{2+} + Fe^{3+} + 2DGL \rightleftarrows [CaFe^{III}H_{-4}DGL_2]^- + 4H^+$

(25) $Ca^{2+} + Fe^{3+} + 2DGL \rightleftarrows [CaFe^{III}H_{-5}DGL_2]^{2-} + 5H^+$

Scheme 1

As can be seen in Fig. 1a and 1b the stoichiometry of the $Fe^{III}DGL$ complexes changes from 1 : 1 to 1 : 2 when the concentration of the ligand *c*(DGL) exceeds *c*(Fe^{3+}). The formation of the species $[Fe^{III}{}_2H_{-7}DGL_2]^{3-}$ which has been proposed in the literature[18] could also be confirmed by the calculations. The formation of the depronated forms of 1 : 1 stoichiometry is in agreement with results published by Pecsok.[14] The formation of a series of 1 : 2 complexes formed at higher concentrations of DGL explains the differences in the results published for $Fe^{III}DGL$, because only 1 : 1 complexes have been considered until now.

In Scheme 1 the reactions for complex formation in the $Fe^{III}DGL$ and $CaFe^{III}DGL$ systems are summarised.

In Fig. 1c and 1d the species distribution for the Ca^{2+} : Fe^{3+} : DGL molar ratios 1 : 1 : 1 and 1 : 1 : 2 are shown.

As long as a molar ratio of 1 : 1 or 1 : 1 : 1 is adjusted in solution complexes of a 1 : 1 and 1 : 1 : 1 stoichiometry are formed (eqn. (2)–(6) and (14)–(19)). The deprotonation of the species is then dependent on the pH, appropriately −log[H^+]. Only in the case of the binary system $Fe^{III}DGL$ is the formation of a binuclear system $[Fe^{III}{}_2H_{-7}DGL_2]^{3-}$ found (eqn. (7)). When DGL is present in higher concentrations 1 : 2 and 1 : 1 : 2 species are formed, which is in agreement with the product isolated by Traube (eqn. (8)–(12) and (20)–(25) in Scheme 1).[13]

At higher concentrations the formation of Ca^{2+} containing complexes can be directly observed in the potentiometric titration curves (Fig. 2).

Experiments 1 and 2 in Fig. 2 show the result of a potentiometric titration of the $Fe^{III}DGL$ complexes. The titration experiment starts after the addition of five equivalents of

Table 2 Composition of solutions investigated in the CV experiments: solution A: $c(Fe^{3+}) = 0.01$ mol dm^{-3}, c(DGL) = 0.02 mol dm^{-3}; solution B: $c(Ca^{2+}) = 0.01$ mol dm^{-3}, $c(Fe^{3+}) = 0.01$ mol dm^{-3}, c(DGL) = 0.02 mol dm^{-3}

	No.	Volume of solution A/ml	Volume of solution B/ml	$c(Ca^{2+})$/mol dm^{-3}
pH = 9		(pH = 9.4)	(pH = 8.9)	
	9–0	10	0	0
	9–4	6	4	0.004
	9–8	2	8	0.008
	9–9	1	9	0.009
	9–10	0	10	0.010
pH = 11		(pH = 10.9)	(pH = 11.4)	
	11–0	10	0	0
	11–4	6	4	0.004
	11–8	2	8	0.008
	11–9	1	9	0.009
	11–10	0	10	0.010
pH = 12		(pH = 12.1)	(pH = 12.2)	
	12–0	10	0	0
	12–4	6	4	0.004
	12–8	2	8	0.008
	12–9	1	9	0.009
	12–10	0	10	0.010

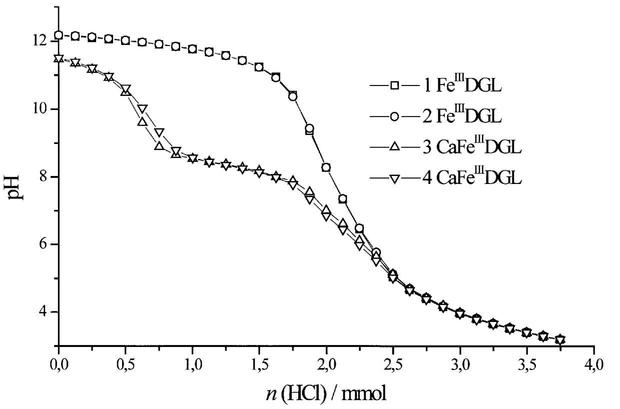

Fig. 2 Potentiometric titrations: (1) and (2) 100 ml solution containing $c(Fe(NO_3)_3{\cdot}9H_2O) = 0.01$ mol dm^{-3}, c(DGL) = 0.02 mol dm^{-3}, c(NaOH) = 0.05 mol dm^{-3}; (3) and (4) in the presence of $c(CaCl_2) = 0.01$ mol dm^{-3}.

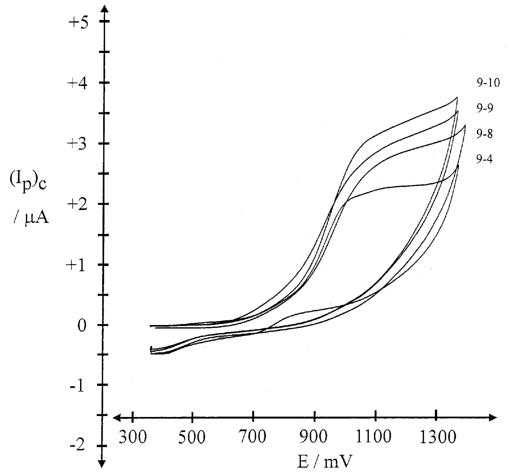

Fig. 3 Cyclic voltammograms of solutions 9–4, 9–8, 9–9, 9–10 ($c(Fe^{3+}) = 0.01$ mol dm^{-3}, c(DGL) = 0.02 mol dm^{-3}, $c(Ca^{2+}) = 0.00$–0.01 mol dm^{-3}), pH 9, in the potential range −360 mV to −1360 mV at a scan rate of 50 mV s^{-1}.

NaOH. $[Fe^{III}H_{-4}DGL_2]^{3-}$ is present in solution as the main complex species. After the addition of 1 equivalent $CaCl_2$ ($c(Ca^{2+}) = 0.01$ mol dm^{-3}) an additional equivalent of NaOH is consumed through the formation of $[CaFe^{III}H_{-5}DGL_2]^{2-}$ (Fig. 2, experiments 3 and 4). The formation of $[CaFe^{III}H_{-4}DGL_2]^{1-}$ occurs in the pH interval from 10 to 7.

These results describing the formed complexes are required as a basis for the understanding and discussion of the electrochemical behaviour of the complexes.

Cyclic voltammetry and batch electrolysis experiments

The changes in the electrochemical properties of the complexes were studied with cyclic voltammetry and batch electrolysis experiments.

In a series of CV-experiments, voltammogramms were recorded for solutions containing $c(Fe^{3+}) = 0.01$ mol dm^{-3}, c(DGL) = 0.02 mol dm^{-3} and $c(Ca^{2+}) = 0$–0.01 mol dm^{-3}. The influence of the pH was studied at pH-values of 9, 11 and 12. The composition of the solutions is given in detail in Table 2. The voltammograms recorded at a scan rate of 50 mV s^{-1} for the different pH values are shown in Fig. 3–5.

In the presence of Ca^{2+} ions a distinct change in the shape of the voltammograms is observed.

pH 11. From the species distribution curves in Fig. 1d the cathodic current maximum $(I_p)_c$ at $(E_p)_c$ −1080 mV can be attributed to $[CaFe^{III}H_{-5}DGL_2]^{2-}$ with a redox reaction according to eqn. (26).

$$[CaFe^{III}H_{-5}DGL_2]^{2-} + e^- \rightleftarrows [CaFe^{II}H_{-5}DGL_2]^{3-} \quad (26)$$

With increasing concentration of Ca^{2+} the CV-curves show an increase of $(I_p)_c$ which indicates the formation of the Ca^{2+}-complex $[CaFe^{III}H_{-5}DGL_2]^{2-}$. A linear relation between the cathodic current and the Ca^{2+} concentration is not observed because following the reduction step according to eqn. (26) redox reactions between cathodically formed $[CaFe^{II}H_{-5}DGL_2]^{3-}$ and non-reduced Fe^{III}-complexes *e.g.* $[Fe^{III}H_{-4}DGL_2]^{3-}$ can increase the cathodic current.[7]

pH 9. From the species distribution shown in Fig. 1d it can be seen that in a solution with pH 9 several species are expected to be present $[CaFe^{III}H_{-3}DGL_2]$, $[CaFe^{III}H_{-4}DGL_2]^-$, $[CaFe^{III}H_{-5}DGL_2]^{2-}$.

The uptake of Ca^{2+} by the Fe^{3+}-complexes causes distinct changes in the shape of the voltammogram and an increase of the cathodic current at a potential of *ca.* −1000 mV. As the current increases with $c(Ca^{2+})$ this reduction can be attributed to the formation of Ca–Fe^{III}–DGL complexes. The cathodic current at $c(Ca^{2+}) = 0.004$ mol dm^{-3} is higher than expected from a linear relation between current and Ca^{2+} concentration, which again can be attributed to coupled redox reactions.[7]

Table 3 Composition of the catholytes used for the constant current electrolysis tests

Experiment	$c(Fe^{3+})$/mol dm^{-3}	c(DGL)/mol dm^{-3}	c(NaOH)/mol dm^{-3}	$c(Ca^{2+})$/mol dm^{-3}	pH-start	pH-end
A	0.1	0.2	0.50	–	12.49	12.79
B	0.1	0.2	0.59	0.1	12.43	12.73

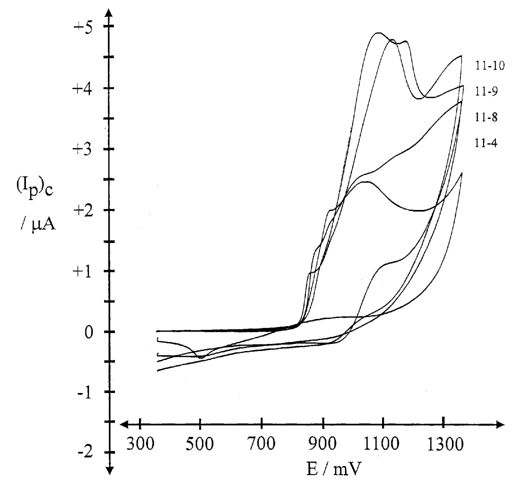

Fig. 4 Cyclic voltammograms of solutions 11–4, 11–8, 11–9, 11–10 ($c(Fe^{3+})$ = 0.01 mol dm^{-3}, c(DGL) = 0.02 mol dm^{-3}, $c(Ca^{2+})$ = 0.00–0.01 mol dm^{-3}), pH 11, in the potential range f −360 mV to −1360 mV at a scan rate of 50 mV s^{-1}.

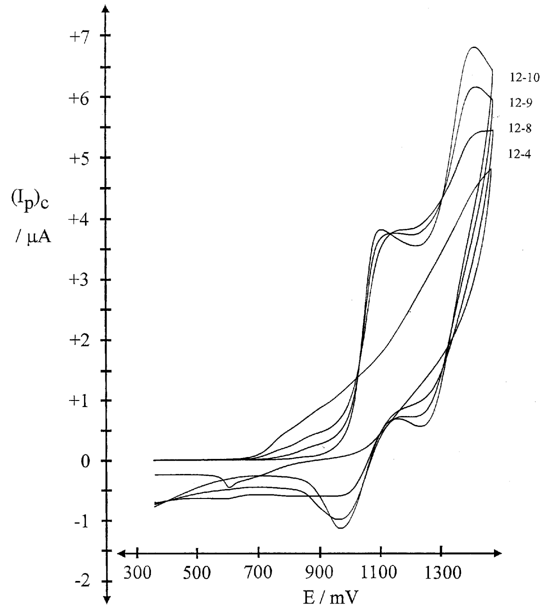

Fig. 5 Cyclic voltammograms of solutions 12–4, 12–8, 12–9, 12–10 ($c(Fe^{3+})$ = 0.01 mol dm^{-3}, c(DGL) = 0.02 mol dm^{-3}, $c(Ca^{2+})$ = 0.00–0.01 mol dm^{-3}), pH 12, in the potential range −360 mV to −1460 mV at a scan rate of 50 mV s^{-1}.

pH 12. At pH 12 besides $[CaFe^{III}H_{-5}DGL_2]^{2-}$ with $(E_p)_c$ = −1080 mV an additional species is detected in the CV with $(E_p)_c$ = −1400 mV. Due to the high pH-value the stoichiometry of this species could not be derived from the potentiometic titrations.

According to the species distribution curves $(I_p)_c$ attributed to the reduction of $[CaFe^{III}H_{-5}DGL_2]^{2-}$ (eqn. (26)) increases from pH 9 to pH 11 and decreases at pH 12 because the concentration of $[CaFe^{III}H_{-5}DGL_2]^{2-}$ is lowered due to the formation of the complex species with $(E_p)_c$ = −1400 mV.

Good linearity of $(I_p)_c$ at $(E_p)_c$ = −1080 mV *vs.* square root of scan rate is observed at all investigated pH-values (Fig. 6). As the cathodic current at this potential is attributed to the irreversible reduction of $[CaFe^{III}H_{-5}DGL_2]^{2-}$ the shape of the graphs for pH 9, 11 and 12 in Fig. 6 is comparable. The absolute height of the cathodic current is different because the concentration of $[CaFe^{III}H_{-5}DGL_2]^{2-}$ varies with pH.

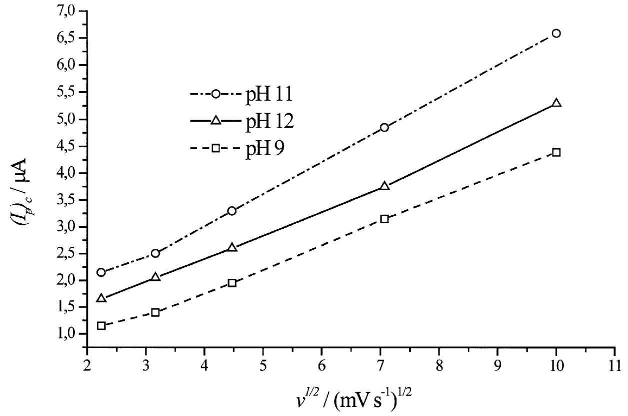

Fig. 6 Dependence of cathodic peak current $(I_p)_c$ ($(E_p)_c$ = −1080 mV) on the scan rate at pH 9, pH 11, pH 12.

To investigate the redox potential formed in solution during cathodic reduction of the complexes constant current electrolysis experiments were carried out with the alkaline solutions of the complexes. In Table 3 the composition of the catholytes A and B used for electrolysis experiments is given. The catholytes were adjusted to the same pH-value before electrolysis to minimise disturbing influences due to the pH-dependence of the redox potential.

Using a divided flow cell a defined amount of Fe^{II}-complex can be formed by cathodic reduction. Starting with the Fe^{III}-form of the DGL-complex part of the complex is reduced to the Fe^{II}-form without distinct changes in the composition of the electrolyte. Parallel to the measurement of the redox potential the ratio Fe^{II} : $Fe^{II/III}$ was determined photometrically using 1,10-phenanthroline.[23]

The slow formation of the Fe^{II}-complex permits the complexes present in the catholyte to achieve chemical equilibrium with regard to the reactions given in Scheme 1. The formal redox potential E measured at the Pt-electrode can thus be understood as a sum parameter describing the redox potential determined by the present set of Fe^{III}- and Fe^{II}- complexes.

Fig. 7 shows the redox potential measured in the different electrolytes A and B as function of the ratio Fe^{II}-form/total $Fe^{II/III}$-complex. As expected from the results of the CV-experiments the uptake of Ca^{2+} causes a distinct shift of the redox potential towards more negative potential values. The formal redox potential measured in the constant current electrolysis experiment for the $Fe^{II/III}$–DGL system is near −600 mV while at the same $Fe^{II/III}$ ratio the Ca–$Fe^{II/III}$–DGL system shows a redox potential of *ca.* −800 mV.

Conclusions

The investigation of the system Ca^{2+}–Fe^{3+}–DGL by potentiometric titration indicates the formation of binuclear complexes with a Ca^{2+} : Fe^{3+} stoichiometry of 1 : 1. Depending on the concentration of DGL complexes with a Ca^{2+} : Fe^{3+} : DGL molar ratio of 1 : 1 : 1 or 1 : 1 : 2 are present. The deprotonation of the complexes is dependent on the pH of the solution. The

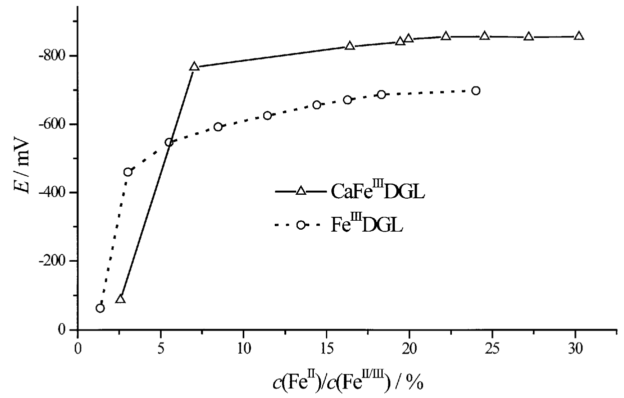

Fig. 7 Change in redox potential as a function of the ratio Fe^{II}-complex/total iron during cathodic reduction of Fe^{III}-complexes. The catholyte composition of experiments A and B is given in Table 3.

formation of the 1 : 1 : 2 complexes is favoured instead of the formation of two separate 1 : 1 complexes *e.g.* CaDGL and Fe^{III}DGL.

The formation of mixed binuclear complexes instead of two different mononuclear complexes (CaDGL and Fe^{III}DGL) provides an explanation for the unexpected finding that Ca^{2+}-ions can change the electrochemical properties of an iron-complex.

The uptake of Ca^{2+} into the complexes causes a distinct change of the electrochemical behaviour of the Fe$^{II/III}$ redox couple which can be demonstrated by CV-experiments. On the basis of the species distribution curves at pH 11 [CaFe^{III}-H$_{-5}$DGL$_2$]$^{2-}$ is proposed as the predominant electrochemically active complex with $(E_p)_c = -1080$ mV. The formal redox potential of the Fe$^{II/III}$DGL complexes is shifted approx. -150 mV towards more negative values by the uptake of Ca^{2+} which can be demonstrated by constant current electrolysis experiments.

Generally the observed shift in formal redox potential caused by an uptake of Ca^{2+}-ions into the Fe$^{II/III}$DGL complexes can be understood as a model for the interaction between an electrochemically inactive ion (Ca^{2+}) and the redox properties of Fe$^{II/III}$-complexes, which thus represents a Ca^{2+}-sensitive redox couple.

Acknowledgements

The authors are indebted to the Fonds zur Förderung der Wissenschaftlichen Forschung (Austria) for financial support of this work (project P 12096-PHY).

References

1 G. Gunasekaran, N. Palaniswamy, B. V. Apparao and V. S. Muralidharan, *Proc.-Indian Acad. Sci., Chem. Sci.*, 1996, **108(4)**, 407.

2 O. Lahodny-Sarc, *Ann. Univ. Ferrara, Sez. 5 Suppl. (1995), 10 (8th European Symposium on Corrosion Inhibitors)*, 1995, **1**, 421.

3 B. J. J. Engbers, *Text. Prax. Int.*, 1992, **47**, 365; B. J. J. Engbers, *Text. Prax. Int.*, 1992, **47**, 462; B. J. J. Engbers, *Text. Prax. Int.*, 1992, **47**, 557.

4 C. L. Mehltretter, B. H. Alexander and C. E. Rist, *Ind. Eng. Chem.*, 1953, **45**, 2782.

5 R. E. Shepherd, Y. Isaacson, L. Chensny, S. Zhang, R. Kortes and K. John, *J. Inorg. Biochem.*, 1993, **49**, 23.

6 T. Bechtold, E. Burtscher, G. Kühnel and O. Bobleter, *J. Soc. Dyers Colour.*, 1997, **113**, 135.

7 S. Mohr and T. Bechtold, *J. Appl. Electrochem.*, 2001, **31**, 363–368.

8 T. Bechtold. and A. Turcanu, *J. Electrochem. Soc.*, 2002, **149**, D7.

9 T. Bechtold, E. Burtscher and A. Turcanu, *Melliand Textilber.*, 2000, **81**, 195.

10 K. Burger and L. Nagy, *Biocoordination Chemistry, Metal complexes of carbohydrates and sugar-type ligands*, ed. K. Burger, Ellis Horwood, Chichester, 1990, ch. VI, p. 236.

11 C. F. G. C. Geraldes and M. M. C. A. Castro, *Metal speciation in the environment, NATO ASI Ser., Ser. G*, ed. J. A. C. Broekaert, S. Gücer, F. Adams, Springer-Verlag, Berlin, 1990, vol. 23.

12 D. M. Whitfield, S. Stoikovski and B. Sarkar, *Coord. Chem. Rev.*, 1993, **122**, 171.

13 W. Traube and F. Kuhbier, *Chem. Ber.*, 1936, **69**, 2655.

14 R. L. Pecsok and J. Sandera, *J. Am. Chem. Soc.*, 1955, **77**, 1489.

15 G. M. Escandar, F. H. Gandolfor and L. F. Sala, *An. Asoc. Quim. Argent.*, 1990, **78(1)**, 37.

16 L. Nagy, L. Burger, J. Kürti, M. A. Mostafa, L. Korecz and I. Kiricsi, *Inorg. Chim. Acta*, 1986, **124**, 55–59.

17 L. Nagy, H. Ohtaki, T. Yamaguchi and M. Nomura, *Inorg. Chim. Acta*, 1989, **159**, 201–207.

18 J. Gonzalez-Velasco, *An. Quim.*, 1980, **76**, 17.

19 A. E. Martell and R. J. Motekaitis, *Determination and Use of Stability Constants*, VCH Publishers, Inc., New York, Weinheim, 2nd edn., 1992.

20 R. J. Motekaitis and A. E. Martell, *Can. J. Chem.*, 1982, **60**, 2403.

21 T. Bechtold, E. Burtscher and A. Turcanu, *Text. Chem. Color.*, 1998, **30(8)**, 72.

22 T. Bechtold, E. Burtscher and A. Turcanu, *J. Appl. Electrochem.*, 1998, **28**, 1243–1250.

23 *Deutsche Einheitsverfahren zur Wasser-, Abwasser- und Schlamm-Untersuchung*, DIN 38406 T1, Wiley-VCH, Weinheim, 1983, Mai, pp. 1–9.

24 R. M. Smith and A. E. Martell, *Critical Stability Constants*, Plenum, New York, 1974, 1975, 1977, 1976, 1982, 1989, vol. 1, 2, 3, 4, 5, 6.